Total cross sections for ultracold neutrons scattered from gases

S. J. Seestrom,[1] E. R. Adamek,[2] D. Barlow,[1] M. Blatnik,[1] L. J. Broussard,[1] N. B. Callahan,[2] S. M. Clayton,[1] C. Cude-Woods,[2] S. Currie,[1] E. B. Dees,[4] W. Fox,[2] M. Hoffbauer,[1] K. P. Hickerson,[5] A. T. Holley,[2,3] C.-Y. Liu,[2] M. Makela,[1] J. Medina,[1] D. J. Morley,[1] C. L. Morris,[1] R. W. Pattie, Jr.,[1] J. Ramsey,[1] A. Roberts,[1] D. J. Salvat,[1,2] A. Saunders,[1] E. I. Sharapov,[6] S. K. L. Sjue,[1] B. A. Slaughter,[2] P. L. Walstrom,[1] Z. Wang,[1] J. Wexler,[4] T. L. Womack,[1] A. R. Young,[4,1] J. Vanderwerp,[2] and B. A. Zeck[4,1]

[1]*Los Alamos National Laboratory, Los Alamos, New Mexico 87545, USA*
[2]*Indiana University, Bloomington, Indiana 47405, USA*
[3]*Tennessee Technological University, Cooteville, Tennessee 38501, USA*
[4]*North Carolina State University, Raleigh, North Carolina 27695, USA*
[5]*California Institute of Technology, Pasadena, California 91125, USA*
[6]*Joint Institute for Nuclear Research, 141980, Dubna, Russia*

(Received 12 July 2016; published 30 January 2017)

We have followed up on our previous measurements of upscattering of ultracold neutrons (UCNs) from a series of gases by making measurements of total cross sections on the following gases hydrogen, ethane, methane, isobutene, *n*-butane, ethylene, water vapor, propane, neopentane, isopropyl alcohol, and ^{3}He. The values of these cross sections are important for estimating the loss rate of trapped neutrons due to residual gas and are relevant to neutron lifetime measurements using UCNs. The effects of the UCN velocity and path-length distributions were accounted for in the analysis using a Monte Carlo transport code. Results are compared to our previous measurements and with the known absorption cross section for ^{3}He scaled to our UCN energy. We find that the total cross sections for the hydrocarbon gases are reasonably described by a function linear in the number of hydrogen atoms in the molecule.

DOI: 10.1103/PhysRevC.95.015501

I. INTRODUCTION

In this paper we describe our efforts to improve on our previous measurement of upscattering of ultracold neutrons (UCNs) from gases [1]. Upscattering results when energy is transferred to the UCN during the scattering process; when this occurs with room-temperature gases the neutrons' energy after collision is essentially always well above the UCN energy range, and the neutron is therefore untrappable in material or magnetic bottles. The motivation, as before, is to use the resulting total cross sections to quantify systematic uncertainties associated with a measurement of the neutron lifetime using stored UCNs, in particular, with the UCNτ experiment [2] currently operating at Los Alamos. The main contaminants in the UCNτ vacuum system are H_2O vapor, oxygen, and nitrogen. In this paper we added water vapor to our previous measurements and determined total cross sections for a series of hydrogen-containing molecules to understand their dependence on the number of hydrogen atoms in the molecule. Since hydrocarbon gases are a potential contaminant in gas systems because of their use in wire chambers, these measurements can be used to predict cross sections for a wide variety of gases. Our improved measurement uses a newly developed UCN [3] detector that can be mounted directly on our gas scattering cell.

II. DESCRIPTION OF THE EXPERIMENT

The experimental configuration is shown in Fig. 1 where the UCNs enter from the UCN source [4] (right). The UCNs can pass through a gate valve [(GV), either open or closed for these measurements] toward the main UCN area. In this experiment, we used a test port which allows a small portion of the beam to pass through an opening of 2.2-cm diameter to a guide section where different experiments can be mounted. Our gas scattering cell is mounted at the end of this section at the bottom of a 1-m drop.

The experimental setup contained two detectors: a detector, which views the main beamline through a small hole to provide a relative UCN fluence monitor (*M* in Fig. 1) and a UCN detector (*D*) after the gas scattering cell. Both of these detectors use a technology recently developed at Los Alamos [3] and are constructed using a plastic sheet coated with a ZnS scintillator powder whose surface is coated with approximately 80 nm of ^{10}B. Neutrons that reach the ^{10}B layer of the detector have a near 100% probability of being captured via $^{10}\mathrm{B}(n,\alpha)\,^7\mathrm{Li}^*$. Because of kinematics, at least one of these particles registers in the ZnS with a high probability. The gas cell was formed from a length of copper UCN guide mounted directly to the front of the detector. The cell had a radius of 3.75 cm and was 12.1 cm in length with the ends defined by a 0.0254-cm-thick aluminum window (10 mil) at the top and the detector at the bottom. The cell was filled with different gas species via a gas manifold, and each species was measured over a range of pressures of $0 < P < 1000$ mbars. The temperature was maintained at $23 \pm 1\,^\circ$C over the course of the experiment.

During these measurements, the UCN source was operated in a pulsed mode with a pulse chain occurring every 5 s (see Ref. [4] for a detailed description of the source operation). The UCNs are extracted from the source through the biological shielding into the very low background experimental area using a UCN guide system with a chicane. This results in

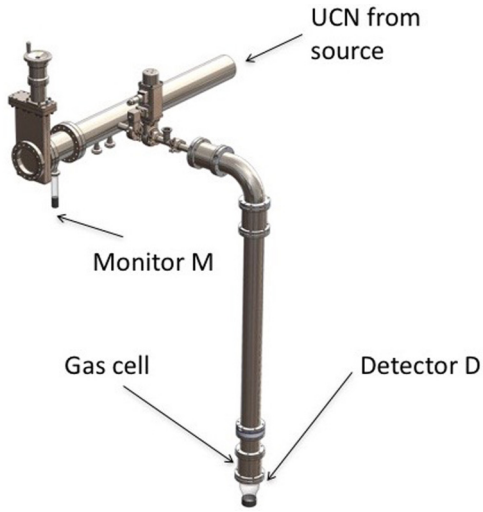

FIG. 1. Experimental layout.

many bounces as the UCNs pass through the guide and thus filter out high-velocity neutrons. The material potential of the stainless-steel guides (189 neV) corresponds to a maximum 609-cm/s velocity for normally incident neutrons, although there is a small tail of neutrons above this energy. The total counts in the detector, coupled directly to the gas cell, were accumulated for 150 s at each pressure; the monitor detector (M) was used to normalize each measurement to variations in UCN production. No appreciable background was observed in the monitor detector, and the monitoring rate was not affected by the presence of gas in the cell. The output of the UCN source was stable within the statistical sensitivity of the monitor normalization.

Yields during each 150-s measurement were extracted from the arrival time spectrum from D and normalized using the background-subtracted counts registered in M during the same time period. The data from D exhibited a constant background; the contribution of the background was estimated from the average of the counts in D over three runs for which the target pressure was sufficient that all UCNs were absorbed.

A. Data analysis

1. Model

The UCN counter D measured the UCNs that were neither absorbed by the gas in the cell nor upscattered and lost from the cell before interacting with the ^{10}B layer. The data are analyzed by making a ratio of the yield at pressure P to the yield at pressure $P = 0$. In particular, the transmission ratio at pressure P is defined in terms of the yield $Y(P)$ as follows:

$$T_n(P) = \frac{Y(P)}{Y(P=0)} = \frac{F\varepsilon[\exp(-\rho_{\rm vol}\sigma_T\bar{l})]}{F\varepsilon} = \exp(-\rho_{\rm vol}\sigma_T\bar{l}). \quad (1)$$

Because of the ratio, there is no need to determine an efficiency or absolute neutron fluence. In Eq. (1) $\bar{l}$ is the average neutron path length through the cell, ε is the detection efficiency for the neutron detector, and F is the neutron fluence φ_n per count $N_{\rm GV}$ in the beam monitor detector M,

$$F = \frac{\varphi_{\rm neutron}}{N_{\rm GV}}. \quad (2)$$

Also in Eq. (1), we define σ_T to be the total cross section for UCN loss due to interaction with the gas,

$$\sigma_T = \sigma_{\rm abs} + \sigma_{\rm up}. \quad (3)$$

$\rho_{\rm vol}$ is the number density of the target gas for a gas temperature of 23 °C and is given approximately by the ideal gas law (we will touch on the impact of nonideal gas behavior when we discuss our error budget),

$$\rho_{\rm vol} = 2.45 \times 10^{16} \times P({\rm mbars})\left(\frac{\rm atoms}{\rm cm^3\ mbar}\right). \quad (4)$$

$\sigma_{\rm abs}$ and $\sigma_{\rm up}$, respectively, are the total cross sections for UCN absorption and upscattering. To a good approximation, both absorption and upscattering result in UCN lifetimes that are independent of velocity because for both processes the first-order cross sections are given by $\sigma_0 = \sigma(v)v$ where v is the UCN velocity and $\sigma(v)$ is the velocity-dependent cross section. When UCN losses are dominated by interaction with the gas, the UCN survival time τ is related to the total cross section,

$$\tau = \frac{1}{\rho\sigma_T v}, \quad (5)$$

where ρ is the number density of the cell given by (4) and σ_T is the total cross section given by (3).

The transport and interaction of the UCNs in our experiment have been simulated using the Monte Carlo transport program UCN [5], which has been benchmarked previously for the characterization of the Los Alamos Neutron Science Center UCN source [4]. The simulation was updated to represent the current experimental configuration. Neutrons are transported from a solid deuterium (SD_2) source to the gas cell accounting for the effect of gravity, the velocity boost the UCNs receive when they leave the Fermi potential of the SD_2, the UCN transport through the guide system, transmission through the gas cell window, and nonspecularity in the UCN scattering from the walls of the cell. Neutrons in the volume of the gas cell are absorbed with a survival time τ, which is a variable in the simulation. A nonspecular component in the UCN scattering from the walls of the cell of 3% was used in the simulation. The main uncertainty in the simulation results from this choice of the size of the nonspecular component, which was taken from Ref. [4]. When the specularity is increased from 3% to 20%, the average path length in the cell increases by 13%; this results in a 13% decrease in the extracted cross section. We have used this range of specularity to estimate systematic uncertainties in our extracted cross sections from this parameter.

The average neutron velocity in the cell $\bar{v}$ and path length to the wall $\bar{l}$ were calculated using our Monte Carlo simulation of the experiment to be 660 cm/s and 15.7 cm, respectively. The average neutron velocity is higher than that at beam height because of the ∼1-m drop to the gas cell. The average path length is longer than the physical length of the gas cell as the UCN can make multiple transits of the cell before they either interact in the gas or encounter ^{10}B at the end of the cell and are captured. Because of the distribution of neutron energies and

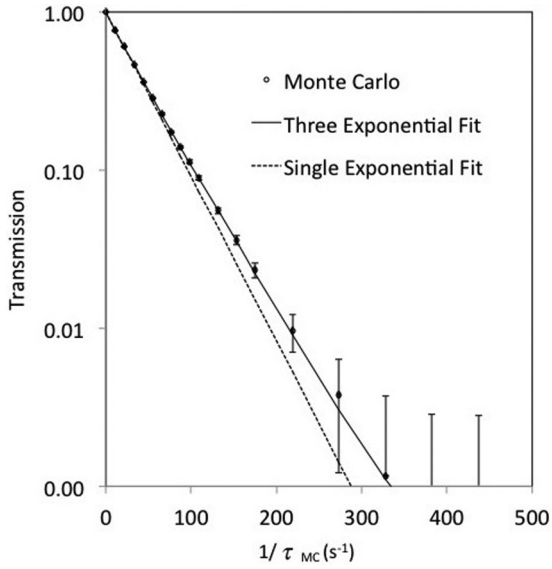

FIG. 2. Fits to the Monte Carlo data where the points are for different UCN survival times in the gas cell using a simple exponential (dotted line) and a triple exponential function (solid line).

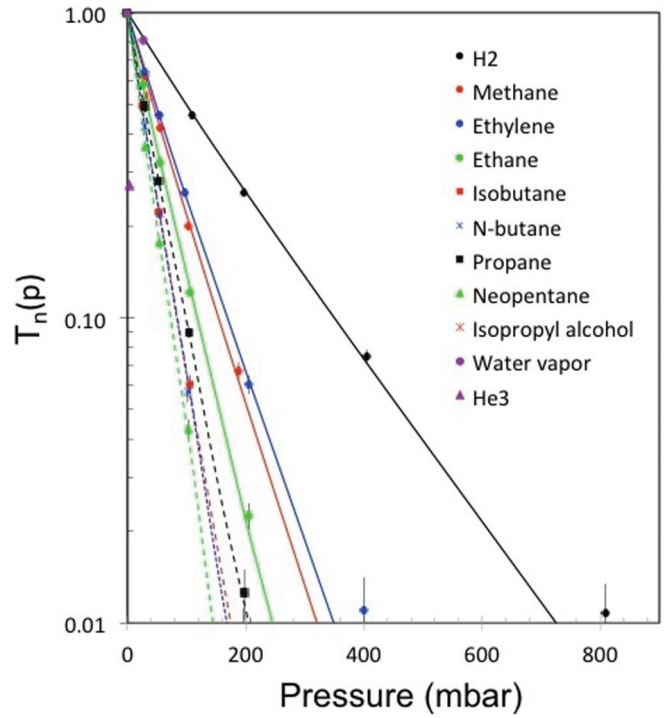

FIG. 3. Transmission ratio plotted as a function of pressure (mbars) along with the fits used to extract the total cross section for each gas.

angles entering the cell, there is a range of different path lengths for UCNs within the cell. We have accounted for expected transport effects in a two-step process. We first simulated the expected transmission ratios as a function of the survival time τ in the cell and then fit the Monte Carlo results to a function that accurately represents the simulated transmissions over the range of τ values explored in our experiment. We then use this functional form (with σ_T and hence τ now the only free parameter) to fit the results of our measurements.

The average transmission resulting from the Monte Carlo simulation is plotted as a function of the inverse survival time in Fig. 2; also shown (dashed line in the figure) is a simple exponential obtained using $\bar{v}$ and $\bar{l}$ from the simulation. Although this describes the Monte Carlo well for long survival times, it fails for short survival times and larger attenuation because of the broad UCN spectrum incident upon the cell. We found that a three-exponential model gave an accurate description of our simulated transmissions over the full range of neutron survival times in our experiment as shown in Fig. 2. The functional form for this model was as follows:

$$T_n = a_1 e^{-(k_1/\tau)} + a_2 e^{-(k_2/\tau)} + a_3 e^{-(k_3/\tau)}. \quad (6)$$

The parameters $(a_1,a_2,a_3,k_1,k_2,k_3)$ were free parameters chosen to give the best fit, subject to the constraint that the a_i sum to unity. The use of three values of l/v is similar to the practice in which a limited number of neutron groups are used to approximate a complex neutron spectrum in many Monte Carlo applications.

2. Fitting

The function in (6) can be used to fit the transmission ratio $T_n(P)$ defined in Eq. (1), varying the total cross section [related to τ by (5)]. The data and resulting fits are shown in Fig. 3. The extracted total cross sections are listed in Table I. The uncertainties in Table I include the statistical uncertainties and the uncertainty due to the fitting procedure.

In addition to the uncertainties due to statistics and fitting we have considered the following potential systematic effects: (1) uncertainty due to errors in the length of the gas cell, (2) uncertainty in the neutron velocity (and hence l/v), (3) uncertainty in gas density, and (4) uncertainty due to the parameters of the Monte Carlo calculation. The uncertainty in the size of the gas cell is estimated to be $\sim$5 mm due to possible bowing of the windows. We estimate the uncertainty in velocity to be due to an error of 2 cm in the vertical drop. We have estimated a 1% uncertainty in the gas density due to our measurement of the pressure (due to the sensor accuracy) and a total of about 1% uncertainty due to our conversion from pressure to density (with 0.3% coming from uncontrolled variations in the temperature over the course of our measurements and 1% coming from nonideal gas behavior for the hydrocarbon species). Based on the previous discussion of the effect on the nonspecular component in the Monte Carlo simulation, we assign a systematic uncertainty of 13% for this source.

The overall systematic uncertainty is 14% with the dominant uncertainty coming from uncertainty about the size of the nonspecular component of UCN scattering in the gas cell. As a test for the presence of a pressure-independent offset in the UCN losses not properly eliminated by the ratio method of Eq. (1), we can use our previous measurement of the smaller upscattering cross sections for the noble-gas species Ne, Ar, and Xe. We determined each of these upscattering cross sections to within about 50 b of what was expected

TABLE I. Total cross sections determined in this paper for a gas temperature of 23 °C and an average UCN velocity of 660 cm/s. Also shown are our previously published total cross sections for H_2 and isobutane [1]. We have also calculated the maximum allowable pressure of each gas needed to achieve an uncertainty in measuring the neutron lifetime of 10^{-4} (equivalent to 0.1 s). Overall systematic uncertainty is 14% except for ^{3}He where it is 34%.

Molecule	σ_T (barns) from this paper	σ_T (barns) from Ref. [1] and ^{3}He scaled from thermal energy	Pressure required for $\Delta\tau_n/\tau_n\|_{\rm loss} = 10^{-4}$ (Torr)
H_2	18500 (300)	20000 (4000)	2.9×10^{-7}
Ethane	55200 (1000)		9.6×10^{-8}
Methane	42000 (500)		1.3×10^{-7}
Isobutane	76800 (1100)	75000 (15000)	6.9×10^{-8}
n-butane	77300 (1,00)		6.8×10^{-8}
Ethylene	38400 (700)		1.4×10^{-7}
Water	20200 (2100)		2.6×10^{-7}
Propane	65400 (600)		8.1×10^{-8}
Neopentane	88,600 (900)		6.0×10^{-8}
Isopropyl alcohol	49900 (3100)		1.1×10^{-7}
^{3}He	1280000 (410000)	1797000	4.1×10^{-9}

theoretically with errors much smaller than the uncertainties quoted in this paper (all greater than 300 b).

^{3}He was measured at a single pressure of 2.8 mb, which is of the same magnitude as the gauge accuracy of 0.6 mb. For this reason we included an additional systematic uncertainty of 30% in the ^{3}He total cross section resulting in an overall systematic uncertainty of 34% in the ^{3}He total cross section.

III. RESULTS

The total cross sections determined for hydrogen and isobutane are in good agreement with those we have previously reported [1] for these gases. In the present data the uncertainty (statistical plus fitting) is smaller than our previous result because of the much simpler fitting procedure. The total cross section determined for ^{3}He is smaller than expected by scaling the known cross section at thermal energies. When the systematics associated with measuring a very low pressure are included, the data are almost in agreement. A measurement for H_2 was also performed in Russia [6] using reactor neutrons. In that paper the data obtained as a function of neutron velocity were fitted as a liner function of velocity. At our velocity of 660 cm/s, the parameters of Ref. [6] yield a cross section of 15 600 (3000) b, in agreement with our result for H_2.

The uncertainty in a measured neutron lifetime τ_n due to a source of neutron loss $\tau_{\rm loss}$ is given by

$$\left.\frac{\Delta\tau_n}{\tau_n}\right|_{\tau_{\rm loss}} = \left(\frac{\tau_n}{\tau_{\rm loss}}\right)\left(\frac{\Delta\tau_{\rm loss}}{\tau_{\rm loss}}\right). \tag{7}$$

We have calculated the partial pressure of each gas that would result in a relative uncertainty of 10^{-4} in the lifetime (corresponding to 0.1 s), assuming that the uncertainty on the loss rate is 100%. These limits are listed in Table I. If the loss rate (i.e., the pressure and total cross section) is known to 20%, then these pressures would result in a relative uncertainty of 2×10^{-5} in the lifetime, sufficient for an overall uncertainty of 0.1 s.

IV. DISCUSSION

The inelastic scattering of slow neutrons is described in theory by the scattering function $S(\mathbf{Q}^2,\omega)$ [7,8] that depends on the neutron energy change in the scattering ($\hbar\omega = E' - E$) and the square of momentum transfer [$\mathbf{Q}^2 = (\mathbf{k}')^2 + (\mathbf{k})^2 - 2k'k\cos\theta$]. Here the bold indicates vector quantities, E' and E are the neutron final and initial energies, respectively, k and k' are the initial and final neutron wave vectors, and θ is the scattering angle. For the hydrocarbon species investigated here, the double differential cross section per molecule can be written as

$$\frac{d^2\sigma}{d\Omega\, dE'} = N_{\rm H}\frac{\sigma_b}{4\pi}\sqrt{\frac{E'}{E}}S(\boldsymbol{Q}^2,\omega), \tag{8}$$

where $N_{\rm H}$ is the number of the H atoms in the molecule, $\sigma_b = 80.2$ b is the incoherent bound-atom scattering cross section for protons, and $S(\mathbf{Q}^2,\omega)$ is the molecular dynamical structure factor averaged over all H atoms in the molecule and having the dimension of (meV^{-1}). Our data (Fig. 4) deviate from a linear dependence on $N_{\rm H}$ above $N_{\rm H} = 6$. It was pointed out in Ref. [9] that the linear dependence on $N_{\rm H}$ (8) is questionable because different H atoms in a given molecule have different bonding and thus scatter neutrons differently. The $S(\mathbf{Q}^2,\omega)$ function contains the complete dynamics of the scattering process, which includes translations of the molecule center of mass, rotations about this center, and vibrations of atoms in the molecule.

Upon integration of $S(\mathbf{Q}^2,\omega)$ over the solid angle and the final energy E' and dividing by $N_{\rm H}$, the total cross section per H atom ($\sigma_{\rm H}$) can be obtained. For neutrons with a sufficiently low initial energy $E \ll \hbar\omega$, the only inelastic scattering is a process where a neutron gains energy from the target. In such a case the integration is simplified because $\hbar\omega = E'$, and the two variables of the function $S(\mathbf{Q}^2,\omega)$ become related by $\hbar\omega = E' = (\hbar Q_*)^2/2m$. The angular distribution of scattering therefore tends to be isotropic. We can express the cross section as a function of wavelength λ. In this notation the total scattering cross section per H atom in molecule as a function

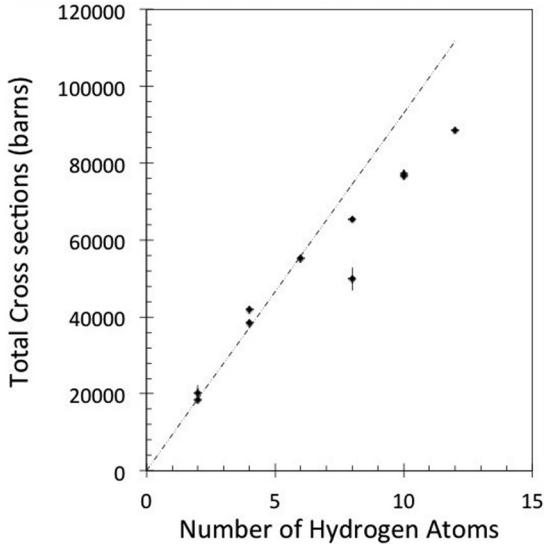

FIG. 4. Total cross section as a function of the number of hydrogen atoms. The line to guide the eye was chosen to go through the origin and the cross section for hydrogen.

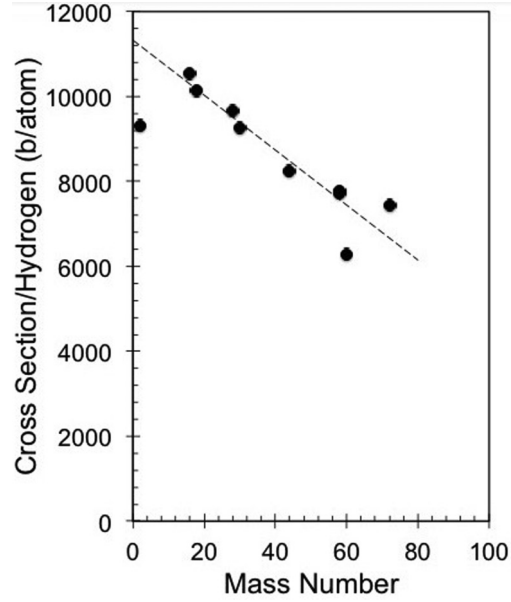

FIG. 5. Cross section per hydrogen atom as a function of molecular mass calculated from our data.

of λ is given by

$$\sigma_{\rm H}(\lambda) = (\lambda)\frac{\sigma_b}{h}\sqrt{2m}\int \sqrt{E'}S(Q_*^2,E')dE'. \qquad (9)$$

This demonstrates the linear dependence of the cross section per H atom on the wavelength; the proportionality will be different for different molecules, depending on the intramolecular dynamics. In principle the slopes $\Delta\sigma_T/\Delta\lambda$(b/Å) can be calculated given specific models for $S(\mathbf{Q}^2,\omega)$. For the CH_4 molecule we use the results of the quantum-mechanical calculation of $S(\mathbf{Q}^2,\omega)$ by Griffing [10,11] and Brugger *et al.* [12] to calculate the integral from which we obtain $\Delta\sigma/\Delta\lambda = 15.9$ (b/Å).

The linear trend in the cross section appears to be valid for $\lambda > 5$ Å as was shown in measurements [10,11] in the wavelength range of 5.5−11.5 Å [13,14]. For example, the species NH_3 slope was found to be $\Delta\sigma_T/\Delta\lambda = 15.5$ (b/Å) per hydrogen atom. The $\sigma_{\rm H}(\lambda)$ values for all hydrocarbon molecules measured by Melkonian [15] are close to 90 b per H atom at $\lambda = 5$ Å. Therefore we have deduced, from our UCN ($\lambda = 600$ Å) cross-sectional measurements, the slopes by taking the ratios $(\sigma_{\rm H} - 90)$ b/(600−5) Å. These slopes are shown in Table II. Within experimental uncertainty the values are the same as the total cross-sectional values of $\sigma_{\rm H}$ divided by $\lambda = 600$ Å, and so they exhibit the same dependence on the molecule mass as shown in Fig. 5 for the total scattering cross section per atom $\sigma_{\rm H}$ vs the molecule mass M. One can qualitatively explain the observed systematic decrease with M by considering Eq. (9) for $\sigma_{\rm H}$ and a general knowledge of the dynamics of measured gaseous molecules. The heavier molecules have a larger contribution of smaller rotational frequencies in $S(\mathbf{Q}^2,\omega)$ which are relatively more suppressed by the factor $\sqrt{E'}$ in the integral of Eq. (9). As opposed to heavy molecules, the light hydrogen molecule has a large contribution from quasielastic scattering (translational modes with small frequencies) which leads also to a smaller value of $\Delta\sigma/\Delta\lambda$.

TABLE II. Slopes of the total cross sections per H atom for our UCN population with an average wavelength of 600 Å.

Molecule	M	$\Delta\sigma_T/\Delta\lambda$ (b/Å)
Hydrogen H_2	2	15.4 (0.5)
Methane CH_4	16	17.5 (0.8)
Water H_2O	18	16.8 (3.5)
Ethylene C_2H_4	28	16.0 (1.2)
Ethane C_2H_6	30	15.3 (1.7)
Propane C_3H_8	44	13.6 (1.0)
n-butane C_4H_{10}	58	12.8 (1.8)
Isobutane C_4H_{10}	58	12.8 (1.8)
Isopropyl alcohol C_3H_8O	60	10.3 (5.2)
Neopentane C_5H_{12}	72	12.3 (1.5)

V. CONCLUSION

We have performed measurements of the total cross sections for UCNs scattered from a number of gases using an improved technique that reduces the overall uncertainties compared to our previous measurements. In the two gases that were measured using both techniques, the results are in good agreement. We have added water vapor, which is a significant contaminant in our ongoing neutron lifetime experiment (UCNτ). In addition, we have studied a number of hydrocarbon gases to understand the scaling with H-atom number $N_{\rm H}$. These measurements allow us to develop a model that yields a conservative estimate of the total cross section for most commonly used hydrocarbons. The slopes of the cross sections $\Delta\sigma/\Delta\lambda$ reveal a systematic decrease vs mass of molecules that is different from what was observed at higher energies. This

decrease can be explained tentatively by the overall dynamics of the neutron-scattering law.

These results demonstrate that any experiment seeking to perform a measurement of the neutron lifetime with an accuracy of 0.1 s must maintain pressures of common contaminant gases, such as hydrogen or water vapor below a few 10^{-7} Torr. The limits for heavy hydrocarbon gases are approximately five times lower, and ^{3}He is by far the most dangerous contaminant of all. These results underscore the need to use extreme caution with respect to the use of detector gases in connection with such experiments. Any experiment seeking to perform a neutron lifetime measurement approaching 0.1-s accuracy will therefore need to maintain a very high vacuum with well-characterized contaminants.

Previous lifetime measurements using stored UCNs have taken different approaches to the issue of UCN loss by interaction with a residual gas in the storage vessel. Pichlmaier *et al.* [16] have performed the most complete analysis using the known thermal cross sections on hydrogen along with the detailed knowledge of the contaminant gases in their vacuum system. Serebrov *et al.* [17,18] corrected their measured lifetime by spoiling their system vacuum and scaling the resulting zero pressure. This method of correction potentially suffers from the problem that it might not correctly reproduce the original mix of contaminant gases in the vacuum system. The results from our paper show that it is necessary to have a clean vacuum and to understand the makeup of the residual gas in the system. We also have shown that it is reasonable to use cross sections measured at higher energies, scaled to UCN energy, to determine the appropriate correction for the residual gases.

ACKNOWLEDGMENTS

This material is supported by the LANL LDRD program, the U.S. Department of Energy Office of Science, Office of Nuclear Physics through LANL DOE Grant No. 2015LANLE9BU and North Carolina State University Grant No. DE-FG02-97ER41042, the U.S. National Science Foundation through Indiana University Grants No. PHY-0969490 and No. PHY-1068712, and North Carolina State University grant NSF Grant No. 1307426.

[1] S. J. Seestrom *et al.*, Phys. Rev. C **92**, 065501 (2015).
[2] D. J. Salvat *et al.*, Phys. Rev. C **89**, 052501 (2014).
[3] Z. Wang *et al.*, Nucl. Instrum. Methods Phys. Res. Sect. A **798**, 30 (2015).
[4] A. Saunders *et al.*, Rev. Sci. Instrum. **84**, 013304 (2013).
[5] C. L. Morris and A. Roberts, Los Alamos National Laboratory Report No. LA-UR-14-23816, 2014 (unpublished).
[6] Y. Y. Kosvintsev, Y. A. Kushnir, V. I. Morozov, and G. I. Terekhov, *Proceedings of the Vth Kiev Conference on Neutron Physics* (AtomInform, Kiev, Russia, 1980), p. 130.
[7] L. Van Hove, Phys. Rev. **95**, 249 (1954).
[8] P. A. Egelstaff and P. Schofield, Nucl. Sci. Eng. **12**, 260 (1962).
[9] H. L. McMurry, Nucl. Sci. Eng. **15**, 429 (1963).
[10] G. W. Griffing, *STI/PUB/62* (IAEA, Vienna, 1963), p. 435.
[11] G. W. Griffing, Phys. Rev. **127**, 1179 (1962).
[12] R. M. Brugger, V. S. Rainey, and H. L. McMurry, Phys. Rev. **136**, A106 (1964).
[13] J. J. Rush, T. I. Taylor, and W. W. Havens, Phys. Rev. Lett. **5**, 507 (1960).
[14] J. J. Rush, T. I. Taylor, and W. W. Havens, J. Chem. Phys. **37**, 234 (1962).
[15] E. Melkonian, Phys. Rev. **76**, 1750 (1949).
[16] A. Pichlmaier, V. Varlamov, K. Schreckenbach, and P. Geltenbort, Phys. Lett. B **693**, 221 (2010).
[17] A. Serebrov *et al.*, Phys. Lett. B **605**, 72 (2005).
[18] A. P. Serebrov *et al.*, Phys. Rev. C **78**, 035505 (2008).